JACS
JOURNAL OF THE AMERICAN CHEMICAL SOCIETY

ARTICLE

pubs.acs.org/JACS

A Multiswitchable Poly(terthiophene) Bearing a Spiropyran Functionality: Understanding Photo- and Electrochemical Control

Klaudia Wagner,[†] Robert Byrne,[‡] Michele Zanoni,[‡] Sanjeev Gambhir,[†] Lynn Dennany,[†] Robert Breukers,[†] Michael Higgins,[†] Pawel Wagner,[†] Dermot Diamond,[‡] Gordon G. Wallace,[†] and David L. Officer*[,†]

[†]ARC Centre of Excellence for Electromaterials Science and Intelligent Polymer Research Institute, University of Wollongong, Northfields Avenue, Wollongong, NSW 2522, Australia

[‡]CLARITY Centre for Sensor Web Technologies, National Centre for Sensor Research, Dublin City University, Collins Avenue, Glasnevin, Dublin 9, Ireland

Supporting Information

ABSTRACT: An electroactive nitrospiropyran-substituted polyterthiophene, poly(2-(3,3″-dimethylindoline-6′-nitrobenzospiropyranyl)ethyl 4,4″-didecyloxy-2,2′:5′,2″-terthiophene-3′-acetate), has been synthesized for the first time. The spiropyran, incorporated into the polymer backbone by covalent attachment to the alkoxyterthiophene monomer units, leads to multiple colored states as a result of both photochemical and electrochemical isomerization of the spiropyran moiety to merocyanine forms as well as electrochemical oxidation of the polyterthiophene backbone and the merocyanine substituents. While electrochemical polymerization of the terthiophene monomer can take place without oxidation of the spiropyran, increasing the oxidation potential leads to complex electrochemistry that clearly involves this substituent. To understand this complex behavior, the first detailed electrochemical study of the oxidation of the precursor spiropyran, 1-(2-hydroxyethyl)-3,3-dimethylindoline-6′-nitrobenzospiropyran, was undertaken, showing that, in solution, an irreversible electrochemical oxidation of the spiropyran occurs leading to reversible redox behavior of at least two merocyanine isomers. With these insights, an extensive electrochemical and spectroelectrochemical study of the nitrospiropyran-substituted polyterthiophene films reveals an initial irreversible electrochemical oxidative ring-opening of the spiropyran to oxidized merocyanine. Subsequent reduction and cyclic voltammetry of the resulting nitromerocyanine-substituted polyterthiophene film gives rise to the formation of both merocyanine π-dimers or oligomers and π-radical cation dimers, between polymer chains. Although merocyanine formation is not electrochemically reversible, the spiropyran can be photochemically regenerated, through irradiation with visible light. Subsequent electrochemical oxidation of the nitrospiropyran-substituted polymer reduces the efficiency of the spiropyran to merocyanine isomerization, providing electrochemical control over the polymer properties. SEM and AFM images support the conclusion that the bulky spiropyran substituent is electrochemically isomerized to the planar merocyanine moiety, affording a smoother polymer film. The conductivity of the freestanding polymer film was found to be 0.4 S cm^{-1}.

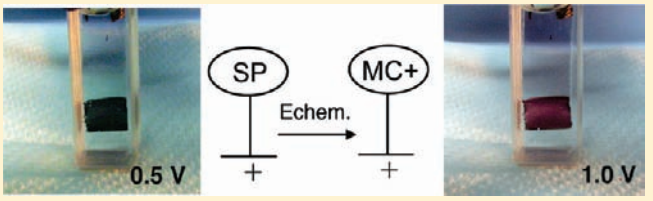

1. INTRODUCTION

The immobilization of light-responsive molecules on electroactive surfaces provides an exciting opportunity for the development of smart materials and devices.[1] Spiropyrans, reported for the first time by Fischer and Hirshberg,[2] are one of the most widely studied classes of photoswitchable compounds. Irradiation of spiropyrans (**SP**, Figure 1) with near-UV light[3] or electro-oxidation[4] induces heterolytic cleavage of the spiro carbon−oxygen bond to produce ring-opened structures (**MC**, Figure 1), represented as two resonance forms, one merocyanine-like and the other quinoidal.

The intense absorption in the visible region of the open form **MC** has led to the advanced study of spiropyrans in photochromic,[5] molecular optoelectronic[6] optobioelectronic fields,[7] and chemical sensing.[8]

The exploitation of such light-responsive molecules in devices typically requires immobilization on a surface through an appended functionality that does not interfere with the light switching behavior. This has been achieved for photoswitchable molecules by formation of self-assembled monolayers (SAMs)[9] and bilayers[10] and incorporation into polymer films[11,12] and beads.[8] While the required structure for monolayer and bilayer formation does not usually affect the function of the photomolecules, one of the challenges in using polymers is that the monomer used to synthesize the polymer, and the polymerization process itself, must be compatible with the photo-/electroactive switching units. In addition, the incorporation of the photoresponsive functionality must not affect the polymerization of the monomer. Wesenhagen et al. recently reported the incorporation of a photo-/electrochromic dithienylcyclopentene moiety into a polymer by oxidative electropolymerization of a methoxystyryl monomer attached to the photoactive unit.[13] The electroactive polymer was formed as only

Received: December 20, 2010
Published: March 18, 2011

   dx.doi.org/10.1021/ja1114634 | J. Am. Chem. Soc. 2011, 133, 5453–5462

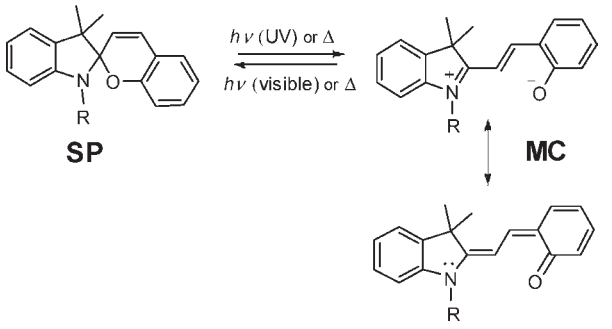

Figure 1. Benzospiropyran (**SP**, left) and its stimuli-induced zwitterionic and quinoidal isomers contribute to the open form (**MC**, right).

a thin film, the thickness of several monolayers as the result of limited conductivity.

The photoswitchable moiety can be appended to the polymer backbone or incorporated into it with quite different effects. In the latter case, the incorporated photoswitchable unit can affect the nature of the polymer backbone. Hugel and co-workers have demonstrated that incorporation of azobenzene units into the backbone of the polymer chain modifies the modulus of elasticity of the polymer.[14] The nature of the polymer backbone can also influence the kinetics of open/closed ring isomerization of the photoactive units, affect the stability, or even lead to enhancement of photo degradation.[15]

While the introduction of photoswitchable molecules into polymers has proved valuable, the use of conducting polymers opens up a new avenue for electrochemical control of these multifunctional materials. In this regard, poly(thiophene) derivatives are of particular interest due to their stability and relative ease of synthesis and functionalization,[16] and they have been applied in a broad range of devices, from simple solar cells[17] to complex electroluminescent devices.[18] This exciting potential of combining photoswitchability and electroactivity together was first recognized by Areephong et al. who reported the ability to control the electropolymerizability of an oligothiophene by the introduction of a photoswitchable dithienylethene unit into the monomer.[19] Most recently, the first spiropyran-functionalized polythiophene was obtained by chemical copolymerization of a thiophene monomer with covalently attached spiropyran and 3-hexylthiophene.[20] In this work, it was demonstrated that both the fluorescence of this photoswitchable conductive copolymer and its interactions with cyanide ions could be controlled through **SP** to **MC** photoconversion. However, the real benefit of combining the photoactivity and electrochemical activity of these materials was not explored.

The introduction of large functionalities onto a polythiophene can have a significant steric effect on the polymer backbone, adversely affecting the optical and electronic properties of the polymer as well as the polymer processability. The use of 4,4″-dialkoxy-3-substituted terthiophenes as a precursor for developing novel substituted poly(thiophene)s provides reduced steric interactions between polymer backbone and substituent, allows better control of polymer regiochemistry, and the alkoxy side chains activate the monomer for polymerization and ensure better polymer processability.[21,22] We have been exploring successfully the polymerization of functionalized dialkoxyterthiophene monomers to avoid these problems.[23] Incorporation of the spiropyran moiety into a dialkoxyterthiophene monomer appeared to provide a good opportunity to investigate the potential for electrochemical control of photoresponsive functionality in a conducting polymer system. In this Article, we report the synthesis and properties of spiropyran-functionalized poly(terthiophene)s. The spiropyran unit is covalently linked to the monomer, which is electropolymerized. The resulting film is electroactive and shows multiswitchable behavior. In this exciting new material, we have electrochemical control of both the polymer redox and the photochemical properties, as well as the ability to convert the **SP** to **MC** form with potential and light. To the best of our knowledge, this is the first report of the synthesis and electrochemical control of electropolymerized conductive polymer film bearing a spiropyran functionality.

2. EXPERIMENTAL SECTION

Experimental details are given in the Supporting Information.

3. RESULTS AND DISCUSSION

3.1. Synthesis of Monomer. The dialkoxyterthiophene acetic acid **TThAA** was chosen in this study as the terthiophene monomer to functionalize with the **SP** group because mild chemistry can be used to form reasonably stable ester linkages with a readily available hydroxyl-substituted spiropyran, such as *N*-hydroxyethylnitrobenzospiropyran **SP1** (Scheme 1). Spiropyran-substituted terthiophene monomer **TThSP1** was readily prepared from the acetic acid **TThAA** (Scheme 1). The precursor methyl acetate **TThMA** was synthesized as previously described[24] and hydrolyzed to give **TThAA** in quantitative yield. Base-catalyzed condensation of **SP1** with **TThAA** afforded **TThSP1** in 77% yield.

The structures of the three substituted terthiophenes are fully consistent with their spectroscopic data. The ^{1}H NMR terthiophene signals are as expected unperturbed by the change in ester functionality with NMR spectral characteristics of **TThSP1** simply being a superposition of the **TTh** and **SP** components.

As expected for nitrospiropyran derivatives, the UV−vis absorption spectrum of **TThSP1** (Figure 2, black line) shows bands in the ultraviolet (not shown) due to the **SP1** substituent. In the visible, the terthiophene absorbance dominates the spectrum at 350 nm, with no absorption due to the merocyanine isomer above 500 nm. Irradiation of a dichloromethane solution of **TThSP1** with UV light leads to the formation of **TThMC1** (Figure 2, violet line), as evidenced by the peak at 564 nm. This is analogous to the photochemical behavior of **SP1** that gives the characteristic peak for a merocyanine at 560 nm (**MC1**, Figure 2, red line). However, an additional band at 446 nm is also observed in the **MC1** spectrum. The origin of this peak has been explained by McCoy et al. who reported that nitro-spiropyran derivatives in dichloromethane isomerize to merocyanines and rapidly form H-aggregates, which exhibit a band at 446 nm.[25]

It seems, therefore, that the terthiophene moiety does not affect the photochromic properties of the spiropyran substituent but does inhibit formation of aggregates.

3.2. Electrochemistry and Spectroelectrochemistry of SP1. Our initial investigations into the electrochemical polymerization of **TThSP1** revealed that the resulting polymer had a more complex electrochemical behavior than expected from a substituted poly(thiophene). Because this behavior clearly arose from the presence of spiropyran, and there appeared to be a limited knowledge of the electrochemistry of spiropyrans

Scheme 1. Synthesis and Polymerization of TThSP1[a]

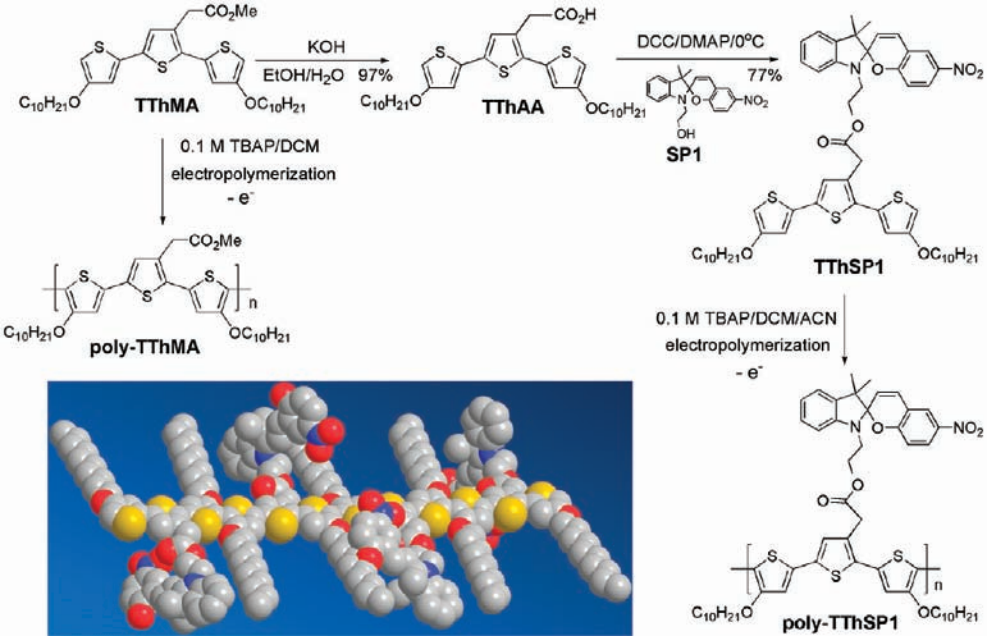

[a] The inset shows a computer-generated model of a short length of the ring-opened merocyanine polymer, **poly-TThMC1**.

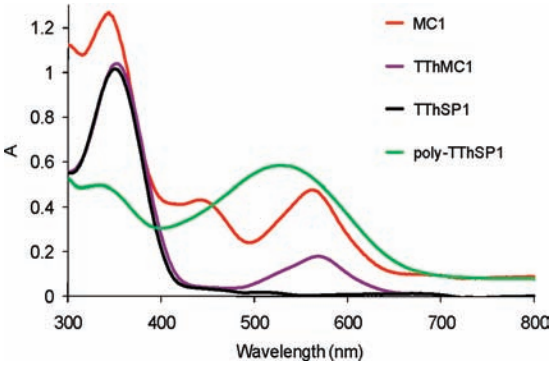

Figure 2. UV−vis spectra of **MC1** after irradiation of **SP1** with 254 nm UV light (red line), monomer **TThSP1** at equilibrium (black line) and when irradiated with 254 nm UV light (violet line), and reduced **poly-TThSP1**. The concentration of **MC1** and **TThSP1** is 1×10^{-4} M in dichloromethane.

generally, we undertook an electrochemical study of **SP1**, which had not been investigated before.

The electrochemistry of analogues of **SP1** has been reported previously.[26−28] Zhi et al. discuss electrochemistry and spectroelectrochemistry of *N*-methylnitrobenzospiropyran, specifically investigating the reduction behavior of the molecule but providing little information about the oxidation of the spiropyran.[27] We do not observe the same electrooxidation characteristics as Zhi and co-workers. Our results are similar to those of Campredon et al.[26] who investigated the electrochemical behavior of naphthalene analogues of **SP1**, although their report includes only a first scan of oxidation voltammograms and a brief comment regarding the instability and possible degradation of the formed radical cation. More recently, Jukes and co-workers[28] reported the electrochemistry and spectroelectrochemistry of 1,3,3-trimethylindolino-6′-nitrobenzopyrylospiran, and, while they report oxidation voltammograms similar to ours, their focus is largely on the reduction influence on the oxidation.

On the first, positive scan on the **SP1** voltammogram (Figure 3a), one irreversible oxidation peak at the potential 0.77 V is observed, with broad, overlapping reduction waves on the reverse scan. It has been proposed that this first oxidation of spiro compounds is a one-electron oxidation at the indoline nitrogen.[4] Because the oxidation is irreversible, a new species must be formed from the oxidized spiropyran. Visual inspection of the solution at the working electrode surface (Figure 3e) during oxidation shows the presence of an orange-red color, similar to that observed by Preigh et al. during electrochemical oxidation of an hydroxyspiropyran and attributed to oxidized merocyanine.[4]

When the **SP1** solution is initially prepared, an equilibrium mixture of the pale yellow **SP1** and red **MC1** forms is clearly present as indicated by the violet coloration (Figure 3c). On standing in the presence of light, this initial equilibrium changes significantly in favor of the **SP1** form, giving the pink color (Figure 3d). Therefore, oxidation at the working electrode is clearly driving the **SP1** to the **MC1** form (red color). Zhi et al. proposed a mechanism for this type of electroisomerization.[27] However, they suggested that the isomerization arises from the reduced spiropyran, which cannot be the case here. As suggested by Preigh and co-workers for an hydroxyl analogue,[4] initial oxidation of the indoline nitrogen to give the $\mathbf{SP}_{ox}$, followed by rearrangement, affords the **MC** radical cation. During the second scan of the CV of **SP1** (Figure 3a), two new broad overlapping oxidation waves appeared with potential maxima at 0.47 and 0.57 V. Because several stereoisomers of the **MC** form have been recognized,[29] the most dominant of which are the TTC (trans−trans−cis) and TTT (trans−trans−trans)[30] forms, it is likely that these peaks may represent the electrochemistry of the two **TTC-MC1** and **TTT-MC1** isomers (Scheme 2). These species themselves could undergo reversible electrochemistry as

dx.doi.org/10.1021/ja1114634 |*J. Am. Chem. Soc.* 2011, 133, 5453–5462

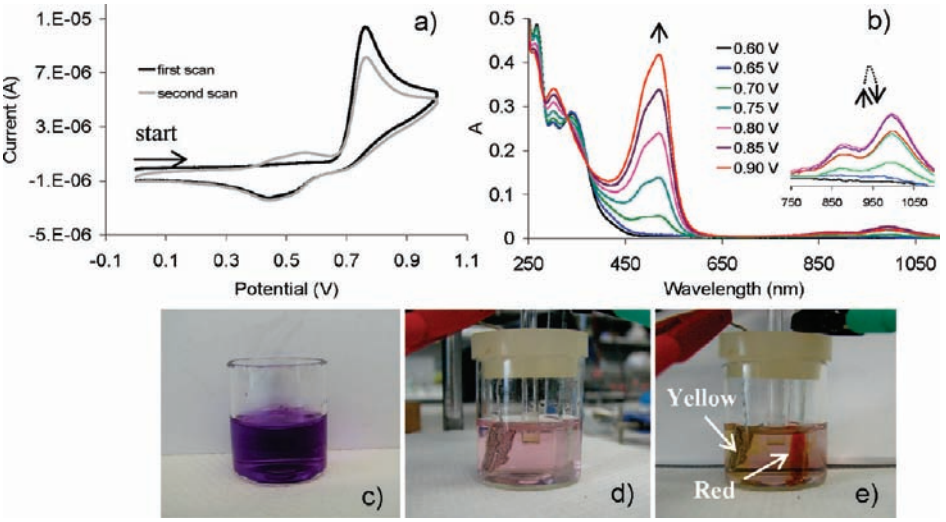

Figure 3. Cyclic voltammograms of **SP1** (a), spectroelectrochemistry during oxidation of 2×10^{-3} M **SP1** in an OTTLE cell (b), a solution of **SP1** just after preparation (c) and after 20 min exposure to visible light (d), and change in **SP1** solution in electrochemical cell during applied potential 1 V to the ITO electrode (e). **SP1** concentrations in (a), (c), d), and (e) are 1×10^{-3} M in acetonitrile with 0.1 M TBAP as electrolyte.

Scheme 2. Postulated Mechanism for the Electrochemical Redox Behavior of SP1

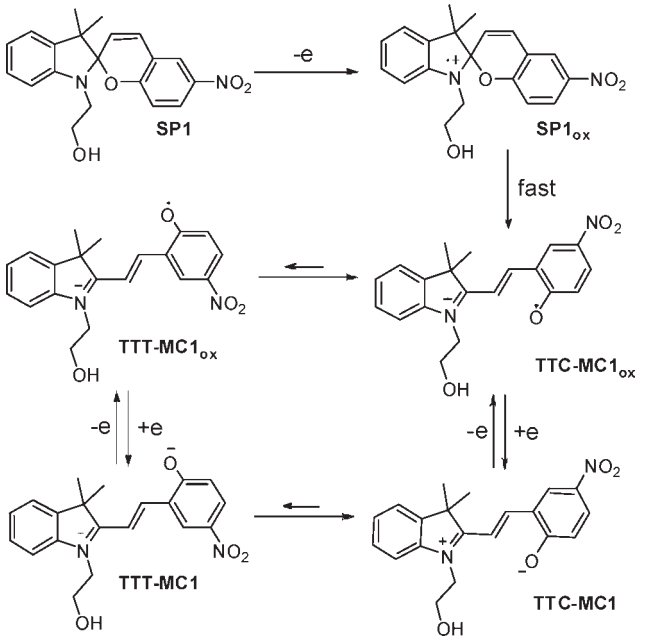

indicated by the reduction peaks at 0.44 and 0.52 V. However, there is no apparent electrochemical path back to **SP1** from either the oxidized or the reduced **MC1** isomers as is indicated by a drop in height of the **SP1** oxidation peak at 0.77 V on the second scan of the CV (Figure 3a).

To further probe this, the absorption spectral changes of **SP1** oxidation processes in 0.1 M TBAP in acetronitrile were recorded at applied potentials from 0.6 to 0.9 V and are shown in Figure 3b. Significant absorbance changes were observed when the potential exceeded 0.65 V, and new absorption bands with maxima at 492 and 523 nm (corresponding to the red solution in Figure 3e) grew rapidly. Therefore, we ascribe these two absorption bands to **TTC-MC1**$_{ox}$ and **TTT-MC1**$_{ox}$. It is also interesting to note the appearance of two absorption peaks at 880 and 997 nm, which rise (0.8 V maximum) and fall as the oxidation potential is increased. Because these peaks reduce in intensity as the amount of **MC1**$^{+}$ increases, we propose that they arise from the formation of **MC1** radical cation dimers. These observations provide significant insights into the electrochemistry and spectroelectrochemistry of **poly-TThSP1**, as we discuss later.

Consequently, we propose that electrochemical oxidation of **SP1** irreversibly leads to isomers of oxidized **MC1**, which themselves undergo reversible electrochemistry as depicted in Scheme 2. Although these are solution-based processes, we anticipated that the spiropyran substituent of **poly-TThSP1** would undergo similar electrochemistry given we had not observed any spectroscopic interaction between the terthiophene and spiropyran groups.

3.3. Electrochemical Polymerization of TThSP1. The electrochemical deposition of **TThSP1** on a platinum disk electrode shows cyclic voltammograms (CVs) with an increase in current with successive cycles, indicative of successful electroactive film deposition (Scheme 1 and Figure 4a). The electropolymerization process is carried out up to 0.8 V, with the onset of monomer oxidation to its radical cation at 0.62 V (inset, Figure 4a) and the formation of bluish film, typical of oxidized polythiophene. We do not observe the characteristic red color of merocyanine at the maximum applied potential of 0.8 V, leading us to conclude that we do not open the spiropyran ring during electrodeposition. The film-coated electrode was placed in monomer-free solution for postpolymerization CV analysis. The post CVs show interesting, dynamic redox behavior (Figure 4b). During the first scan in the post CV of **poly-TThSP1**, three oxidation peaks are visible at 0.12, 0.34, and 0.76 V (Figure 4b). While the origin of the peak at 0.12 V is not clear, the 0.34 V peak can be assigned to oxidation of the polymer backbone (**poly-TTh**$_{ox}$**SP1**, Scheme 3), because cycling of the **poly-TThSP1** film between −0.4 and 0.5 V shows consistent capacitive behavior over more than 10 cycles (not shown). A similar oxidation peak is observed for a **poly-TThMA** film (Figure 4c), which is the analogous spiropyran free polymer,

dx.doi.org/10.1021/ja1114634 |*J. Am. Chem. Soc.* 2011, 133, 5453–5462

with a methyl substituent instead of the nitrobenzospiropyran. In contrast, the sharp oxidation peak at 0.76 V on the first post CV scan of **poly-TThSP1** (Figure 4b) is completely lost during the second scan, but appears to recover somewhat during cycling. The position of this peak is at the same potential as the first oxidation of the **SP1** molecule (Figure 3a). It is likely that the oxidation peak at 0.76 V for **poly-TThSP1** results from loss of an electron from the indoline nitrogen of the **SP1** substituent, leading to the oxidized **MC1** substituent on the oxidized polythiophene backbone (**poly-TTh$_{ox}$MC1$_{ox}$**, Scheme 3).

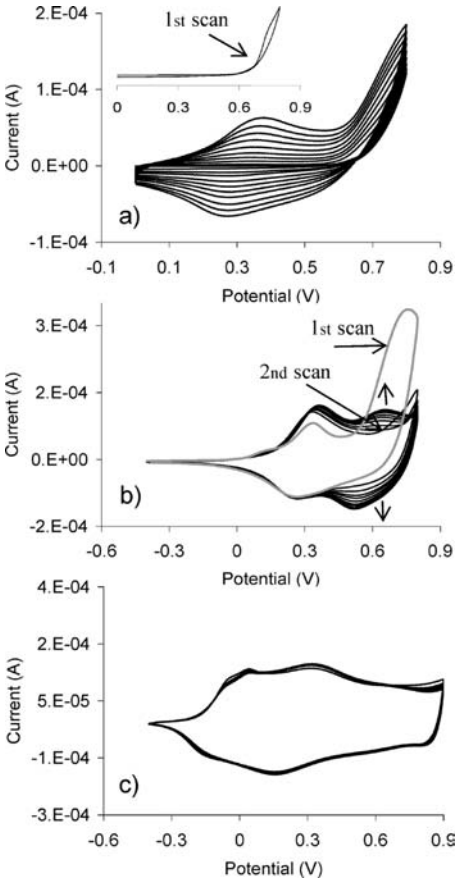

Figure 4. Electrochemical deposition of **TThSP1** with inset showing the first scan (a), post CV voltammograms of **poly-TThSP1** (b) and **poly-TThMA** (c) on platinum disk electrodes, 10 scans at a scan rate 100 mV s^{-1}.

We also observed that the choice of the switching potential used during electropolymerization of **poly-TThSP1** (Figure S1a, c,e) influences the electrochemical characteristics of the post CV voltammogram (Figure S1b,d,f). When the switching potential of electropolymerization is set higher than 0.9 V (Figure S1e), somewhat higher than the oxidation potential of spiropyran **SP1** (0.77 V, Figure 3a), the sharp oxidation peak at 0.76 V on the first post CV scan of **poly-TThSP1** is no longer observed. Clearly, from these post CVs, the oxidation of the appended spiropyran is not reversible, and therefore it appears likely that the substituent on **poly-TThSP1** remains in the **MC** form following further cycling. The CV following initial **poly-TThSP1** oxidation (second scan, Figure 4b) has no peak due to **SP** oxidation, but subsequent scans exhibit a peak at 0.65 V of increasing intensity. This could arise from the oxidation of the polymer **MC** stereoisomers, analogous to that postulated for **SP1** (Scheme 2).

This oxidative electroisomerization of **poly-TThSP1** is also supported by the dramatic color changes observed on oxidation of the polymer film. Polythiophene films generally exhibit two colors, depending on the doped state. For example, the color of the parent poly(terthiophene) in the reduced state is orange-red and brown-black when the polymer is oxidized.[31] Reduced **poly-TThSP1** film is a violet-pink color, but on oxidation to 0.5 V (polymer backbone oxidation) the color changes to green-blue (Scheme 3). Further oxidation to 0.8 V generates a more intense violet-pink film as the result of the formation of the oxidized **MC** substituent. This additional color change at the positive potential occurs very quickly, over a narrow range of potentials (see movie in the Supporting Information). This unique photochromic behavior in the doped state was further investigated using spectroelectrochemistry.

3.4. UV−Visible Spectroelectrochemistry of poly-TThSP1. The spectral properties of **poly-TThSP1** were examined across the potential range used for the post-CV analyses (−0.35 to 0.9 V). **Poly-TThSP1** exhibited typical polythiophene behavior as the electrode potential was increased from −0.35 to 0.6 V, with initial polaron band formation (870 nm) followed by the development of a free carrier tail (Figure 5a). As the applied potential increases from 0.6 V, the growth of a new absorbance at 540 nm is observed (Figure 5b), which corresponds to the initial sharp oxidation shown in the post CVs (Figure 4b). This absorbance is in a position similar to that observed for the photoisomerized **TThMC1** monomer (Figure 2, violet line), and therefore we attribute it to the oxidized **MC** isomer of **poly-TTh$_{ox}$MC1$_{ox}$**.

Scheme 3

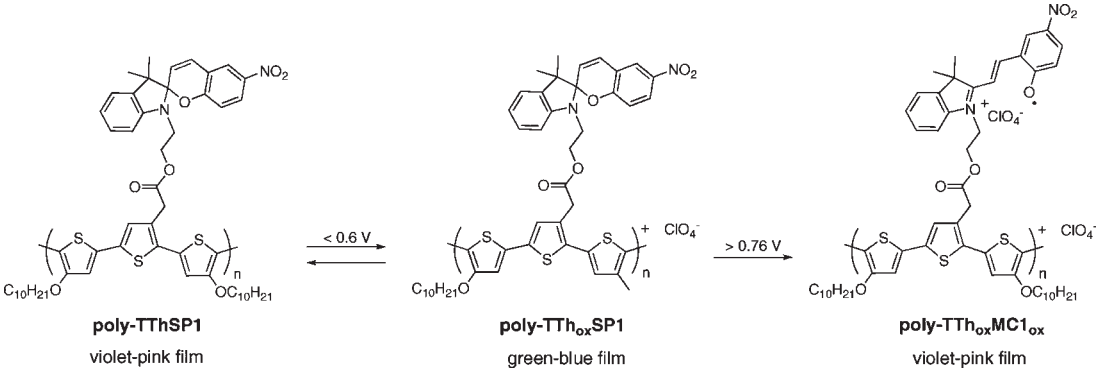

dx.doi.org/10.1021/ja1114634 |J. Am. Chem. Soc. 2011, 133, 5453–5462

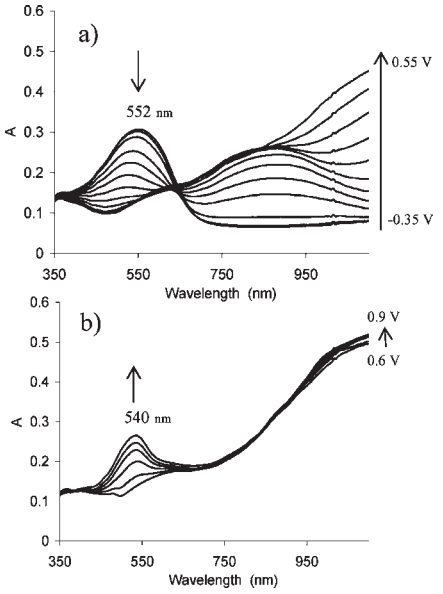

Figure 5. Spectroelectrochemistry of electrochemically polymerized film of **poly-TThSP1** (a and b) on ITO glass for potential ranges of −0.35 to 0.55 V (a) and 0.6−0.9 V (b).

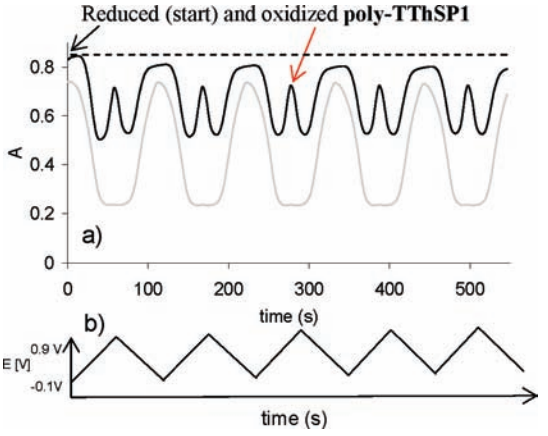

Figure 6. Absorption spectra response at 540 nm for (a) **poly-TThSP1** (black line) and **poly-TThMA** (gray line), when the applied potential was changed from −0.1 to 0.9 V in 0.1 M TBAP in acetonitrile (b).

To probe the reversibility of this merocyanine formation and oxidation, we monitored the 540 nm absorbance over the potential range −0.1 to 0.9 V during cyclic voltammetry (Figure 6). A freshly electrodeposited film was utilized to ensure that the polymer was in the **SP** form. In addition, the same experiment was carried out with a freshly prepared **poly-TThMA**. As seen in Figure 5a, the absorbance at the potential −0.1 V results from the polymer backbone, and, as the polymer becomes oxidized, the absorbance decreases (Figure 6a, black line). When the potential applied to the **poly-TThSP1** film is more positive than 0.6 V, the absorbance at 540 nm increases rapidly as a result of **MC** isomer formation. In contrast, **poly-TThMA** film (Figure 6a, gray line) does not show any absorbance changes at the positive potential range, as is expected for a poly(thiophene).

We also observed following **poly-TThSP1** oxidation for the first time (t = 0, Figure 6a), the same level of absorbance on rereduction (dashed line, Figure 6a), indicative of the formation of ring-opened merocyanine isomers that do not ring close to spiropyran on reduction. This observation is consistent with the variable electrochemical response of **poly-TThSP1** (Figure 4b).

To better understand these changes, a spectroelectrochemical study of fresh films of both **poly-TThSP1** (Figure 7) and control sample **poly-TThMA** (see Supporting Information, Figure S2) was undertaken. The aim of these measurements was to monitor the absorbance changes during a "simulation" of the film cycling. The absorbance spectra in the previous spectroelectrochemical study (Figure 5) only show the initial changes that occur following the oxidation of the spiropyran moiety. In this study, absorbance spectra were obtained while holding the potential at −0.1, 0.6, 0.8, and 1.0 V (Figure 7a−d), potentials at which new peaks appeared in the post-CVs during film cycling (Figure 4b and c). This was repeated six times, effectively mimicking six CV cycles.

Again, it is clear that the spectra recorded during the first "cycle" are different from all the others. Thus, the first spectrum of the reduced **poly-TThSP1** film (Figure 7a) is different across the whole spectrum from the next five spectra recorded at that potential (−0.1 V), consistent with the single wavelength observation evident in Figure 6a. As expected up to 0.6 V, the polythiophene backbone appears to be oxidized, as evidenced by the complete loss of the absorbance at 500 nm as well as the rise of the polaron band at 850 nm (Figure 7b). However, the "second cycle" shows the rise of a new band below 500 nm, which appears to come from the opening of the spiropyran.

The picture becomes clearer from the absorbance spectra at 0.8 V (Figure 7c) and 1.0 V (Figure 7d). The first spectrum at 0.8 V is again assigned essentially to the oxidized polymer backbone, which now shows a significant free carrier tail above 700 nm. The second and later spectra exhibit much more character with two new peaks at 443 and 477 nm and broad absorbances at 870 and 995 nm. All of these bands are then either lost completely or reduced substantially at higher oxidation potential (1.0 V, Figure 7d), with the appearance of a new band around 540 nm and the retention of the free carrier tail.

Therefore, the two bands at 443 and 477 nm are clearly not due to the fully oxidized polymer with oxidized merocyanine, which absorbs at 540 nm. A clue to the origin of these bands lies in the simultaneous appearance of the broad near-infrared absorbances that are almost identical to those observed in the spectroelectrochemistry of the oxidized parent spiropyran **SP1** (Figure 3b). All of these bands appear to arise from the **SP** substituent because an identical spectroelectrochemical experiment involving **poly-TThMA** (see Supporting Information, Figure S2) does not show peaks at 443 and 477 and at 870 and 995 nm following initial polymer oxidation. Because the merocyanine groups are fixed in space by the polymer backbone, the formation of large aggregates is unlikely. However, interaction of two merocyanines with antiparallel dipoles could arise from merocyanines on neighboring polymer chains forming π-dimers. The two peaks at 443 and 477 nm (Figure 7c) could represent dimers formed from the two major merocyanine isomers TTC and TTT (see Scheme 2).

The removal of a single electron from this type of π-dimer to form a π-radical cation dimer might then be expected to be easier than oxidation of a single merocyanine substituent. The formation of π-radical cation dimers in aromatic species is well established in the literature.[22,32,33] Both the spectroelectrochemistry of **SP1** solutions (Figure 3b) and that of the **poly-TThSP1**

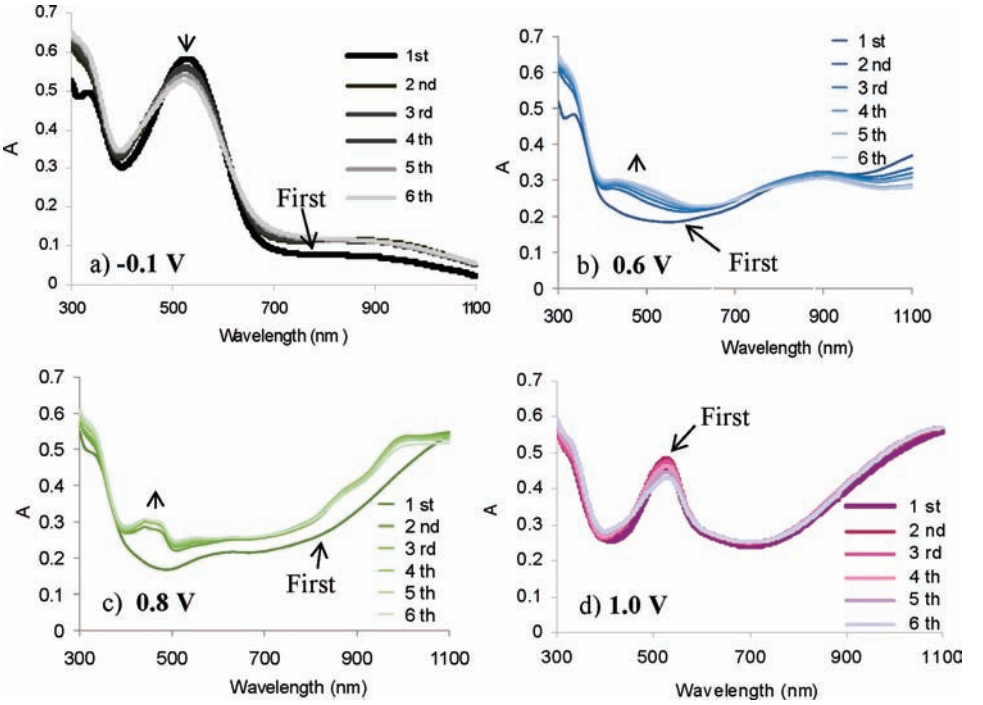

Figure 7. Spectroelectrochemistry of **poly-TThSP1** on ITO recorded six times at the potentials −0.1 V (a), 0.6 V (b), 0.8 V (c), and 1.0 V (d).

film (0.8 V, Figure 7c) are fully consistent with the formation of merocyanine π-radical cation dimers. In both cases, the oxidation of the merocyanine moiety leads to low intensity, longer wavelength peaks between 800 and 1100 nm, that rise and fall as the intensity of the oxidized merocyanine band around 500 nm increases. This can be accounted for by the initial formation of π-radical cation dimers at a low concentration of oxidized merocyanine followed by disappearance of the dimer with complete oxidation of the merocyanine.

The presence of neutral or charged dimeric species or even larger aggregates as a result of merocyanine formation and oxidation accounts for the majority of changes seen in the spectroelectrochemical experiments. To clarify this, we have depicted the processes occurring during the first and subsequent electrochemical cycles in cartoon fashion in Scheme 4.

The left-hand side of the scheme represents the oxidation component of the first cycle with initial polymer oxidation, followed by formation of oxidized spiropyran that rapidly ring opens above 0.8 V to oxidized merocyanine. The reduction component of the first cycle (going up the right-hand side of Scheme 4) leads ultimately to a neutral merocyanine-substituted polythiophene that contains both single, as well as dimeric (or oligomeric), merocyanines. This accounts for the loss of peak height and the peak broadening in the second and subsequent spectra of the spectrochemical study at −0.1 V (Figure 7a). As the polymer is oxidized and reduced, more ordering of the film occurs as a result of strong π-radical cation dimer coupling, leading to an overall increase in neutral dimer formation (and hence peak broadening due to increasing absorptions around 446 nm). This also may explain the apparent increased difficulty in reducing the polymer after the first cycle as evidenced by the increased polaron band at 850 nm.

On the second cycle, it is now the presence of merocyanine π-dimers that dominates the electrochemistry (down the right-hand side of Scheme 4). Oxidation of the merocyanine polymer

Scheme 4. Cartoon Representation of Redox Cycling and Aggregation of poly-TThSP1

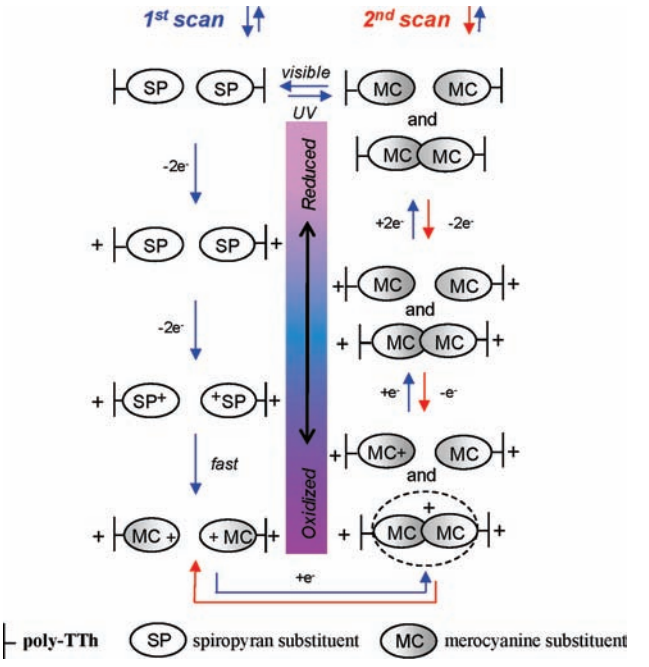

at 0.6 V (Figure 7b) leads to the loss of the neutral polythiophene absorption at 552 nm, revealing broad absorptions from 400 to 550 nm that reflect the presence in the oxidized polymer film of both free merocyanine substituents, as well as merocyanine π-dimers and possibly higher oligomers. Further oxidation (0.8 V, Figure 7c) now gives the characteristic bands of both π-dimers

dx.doi.org/10.1021/ja1114634 |J. Am. Chem. Soc. 2011, 133, 5453–5462

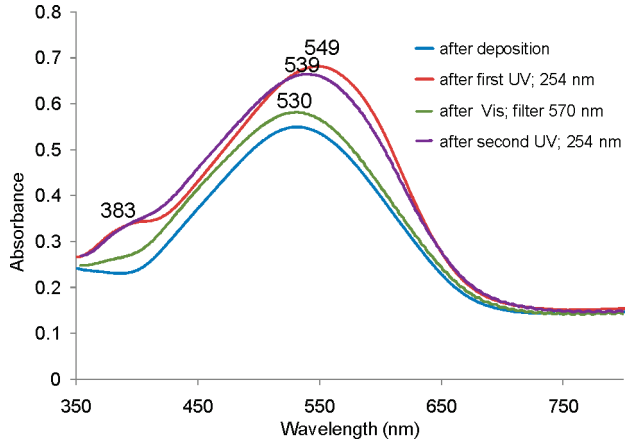

Figure 8. UV−vis spectra of reduced **poly-TThSP1** after electrochemical deposition (blue line), after first irradiation with 254 nm UV light (red line), followed by irradiation with visible light (green line), and second irradiation with 254 nm UV light (violet line).

and π-radical cation dimers as well as both oxidized (~540 nm) and neutral merocyanines (~560 nm) on the oxidized polymer backbone. Finally, full oxidation of the merocyanine groups above 1.0 V (Figure 7d) leads to separation of the merocyanines with only the oxidized merocyanine band at 540 nm apparent in the spectrum.

Given that the spiropyran cannot be regenerated electrochemically, we investigated the feasibility of photochemical control of this process to achieve complete reversibility of this intriguing redox system.

3.5. Light Control of SP1 Isomerization. The photochemical conversion of merocyanine to spiropyran is typically an easily identifiable process, as we observed in the study of **SP1**, because the merocyanine absorption spectrum is largely well separated from the spiropyran spectrum. However, in the case of **poly-TThMC1**, the merocyanine absorption (assumed to be around 560 nm as for **TThMC1**) is at wavelengths similar to that of the reduced polyterthiophene backbone (380−670 nm), making identification of merocyanine formation difficult.To ensure the presence of spiropyran in the polymer, a thin film (<1 μm) of **poly-TThSP1** on ITO glass was CV electrodeposited between 0 and 0.75 V (see Figure S1a), and its UV−visible spectrum was recorded (Figure 8, blue line), following washing to ensure the absence of excess monomer from the polymerization. Irradiation of the dried film with ultraviolet (UV) light (254 nm, 5 min) afforded a more intense and broad UV−visible band (Figure 8, red line) shifted by 20 nm. This is consistent with the formation of **poly-TThMC1**, because the intensity of the polythiophene backbone absorption would be expected to remain constant but the growth of a new absorption centered around 560 nm would lead to a more intense broader band overall. A small broad absorption at 383 nm also appears due to the MC formation. Subsequent irradiation of the polymer film with visible light (40 min) gave a polymer absorption band (Figure 8, green line) identical to that of **poly-TThSP1**, albeit with a slightly higher intensity. A second UV light illumination returned the higher wavelength absorption (Figure 8, violet line), again with small intensity differences. These intensity changes may well be due to conformational changes to the polymer backbone as a result of the spiropyran to merocyanine isomerization.

To ensure that these spectral changes largely resulted from spiropyran to merocyanine isomerization, irradiation of the control polymer **poly-TThMA** was investigated. No change in the absorption spectra of **poly-TThMA** was observed (see Supporting Information, Figure S3) following exposure of polymer film to UV light.

While these experiments demonstrate that the reduced **poly-TThSP1** film, whose SP substituent has never been electrochemically oxidized, undergoes the typical reversible **SP** to **MC** isomerization (Figure 1), further experiments were undertaken to determine whether this was the case for a **poly-TThSP1** film in which the isomerization of the SP moiety had occurred (through irradiation). **TTh-SP1** was electrochemically polymerized on optically transparent ITO-coated glass by chronoamperometric deposition at constant potential (0.8 V) in the dark. At this potential as shown in Figure S1a, the SP substituent should not be substantially oxidized to MC. The **poly-TThSP1** film was then exposed to UV light at 254 nm for 5 min, and the post-CVs (from −0.4 to 0.9 V) obtained with the UV light were still applied to the polymer film (Figure S4a). As expected, no initial electrochemical response ascribed to the spiropyran moiety is observed, suggesting that under these conditions the spiropyran is all converted to merocyanine, giving **poly-TThMC1**. However, in contrast to the previous experiment that only involved photoisomerisation, the **poly-TThMC1** will have been electrochemically oxidized (both polymer backbone and MC substituent) during the post-CV cycling, giving π-cation dimers and other aggregates. The polymer film was then irradiated with visible light (390−750 nm) for 5 min, and the CVs again were recorded over the same potential range while maintaining the visible light irradiation (Figure S4b). Clearly, there is some photochemical regeneration of spiropyran in the film, as evidenced by the appearance of a new peak at 0.55 V in the first CV scan, and its subsequent loss in the second scan. The amplitude of the peak is low, suggesting that only a fraction of the merocyanine substituents in the film are isomerized. Given that the **poly-TThMC1** film is likely to be composed of both free and aggregated merocyanine substituents following oxidation, spiropyran formation would be expected to be sterically limited. In addition, the isomerization must be slow, certainly slower than the time frame of the cyclic voltammetry, because almost no spiropyran is reformed during the subsequent CV scans. This is perhaps not surprising because the reduced merocyanine film would be much more compact than that of the reduced spiropyran film, particularly with increased formation of π-dimers, making it sterically and energetically more difficult to reform spiropyran.

3.6. Physical Properties of poly-TThSP1. It is well-known that conducting polymers display actuation behavior under an external redox potential, due to the movement of counterions and associated solvent molecules into and out of the polymer, which results in swelling and contraction.[34] According to our earlier spectroelectrochemical study, the initial oxidation of the spiropyran moiety provides some merocyanine dimer or oligomer aggregates within the polymer film. These processes should markedly affect the morphology of **poly-TThSP1**, and for this reason scanning electron micrograph (SEM) analysis of the different redox stages of the polymer was undertaken. SEM images were obtained for four **poly-TThSP1** samples electropolymerized in the same way but then subjected to different redox conditions. Three of those samples were oxidized or reduced at constant potential for 2 min. The first image

dx.doi.org/10.1021/ja1114634 |*J. Am. Chem. Soc.* 2011, 133, 5453–5462

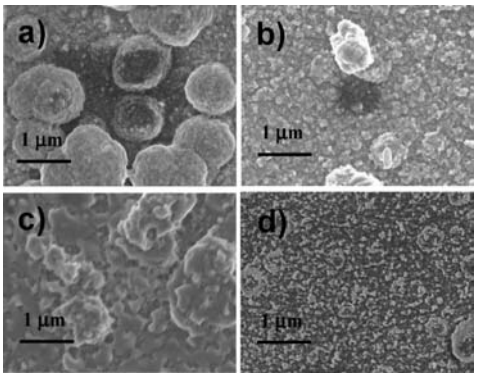

Figure 9. SEM images of **poly-TThSP1** after a constant potential deposition of 0.8 V (a), oxidation at 0.5 V (b), oxidation at 0.85 V (c), and reduction at −0.4 V (d).

in Figure 9a shows the morphology of the fresh film, obtained after 1 min constant potential deposition at 0.8 V. The second polymer sample was oxidized at 0.5 V (Figure 9b) from which we expect only polymer backbone oxidation, while the third one was further oxidized to 0.85 V (Figure 9c), leading to oxidation of the spiropyran substituent on the polymer backbone. The last sample was reduced with the potential −0.4 V (Figure 9d). The morphology of the fresh **poly-TThSP1** (Figure 9a) shows a globular structure, with features approximately 1 μm in diameter present on the polymer surface. Because the polymer backbone is oxidized with associated perchlorate anions and the bulky spiropyran is still present, this film would be expected to show the most expanded morphology. The film oxidized state at 0.5 V (Figure 9b) showed a similar morphology with fewer of the island-particles present on the surface. This would be consistent with the loss of some of the spiropyran groups following the initial film preparation. Significantly, further oxidation of the polymer to 0.85 V (Figure 9c) gave a film with an entirely different morphology with a distinctive webbed and close-packed structure, consistent with the formation of at least partially oxidized planar merocyanine.

AFM images confirm the major change in polymer structure that occurs when the **poly-TThSP1** film is oxidized (Figure S5), because the calculated surface roughness of the reduced (root mean squared, rms = 181 ± 8.4 nm) and oxidized (127 ± 5.1 nm) **poly-TThSP1** suggest a more porous surface for the reduced polymer, as would be expected for the more bulky **SP** substituent.

To measure the conductivity, a free-standing film of **poly-TThSP1** was obtained after chronoamperometric deposition on ITO-coated glass at a constant potential of 0.8 V for 1 h and removal from the electrode. A conductivity of 0.4 S cm^{-1} was obtained, the same order of magnitude as that reported by Gallazzi et al. for an analogous poly(alkoxyterthiophene) substituted with the somewhat smaller electron-withdrawing dicyanoethenyl group.[35]

4. CONCLUSION

The integration of the photochromic properties of spiropyrans with the electrical and optical properties of polythiophenes presents exciting opportunities for a variety of applications. This inspired us to successfully electropolymerize, for the first time, a terthiophene monomer modified with a nitrospiropyran substituent. The resulting polymer, **poly-TThSP1**, displayed a number of different colored states on electrochemical redox cycling with associated complex electrochemistry. To understand this, we undertook a detailed electrochemical study of the nitrospiropyran precursor **SP1** because little had been reported in the extensive spiropyran literature. We have shown that **SP1** initially undergoes irreversible electrooxidative ring-opening to give at least two oxidized merocyanine isomers, which can further undergo reversible redox processes. This behavior is reflected in the electrochemical processes observed for **poly-TThSP1**. The polymer is initially formed with the spiropyran intact and can undergo typical polythiophene redox cycling at potentials below 0.6 V. However, oxidation of the polymer film above 0.8 V leads to spiropyran oxidation and irreversible isomerization to the oxidized merocyanine. A detailed spectroelectrochemical study of the resulting reduction and further redox cycling revealed that the electrochemical and physical properties of the polymer are then dominated by the presence of the merocyanine and its ability to form π-dimers or oligomers and π-radical cation dimers.

The photochemical behavior of **poly-TThSP1** is dramatically influenced by the electrochemistry. Typical spiropyran to merocyanine isomerization within the polymer occurs only if the polymer film has been exposed to oxidation potentials, which do not oxidize the spiropyran moiety to the merocyanine (below 0.8 V). Once the merocyanine is oxidized, the photochemical behavior of the film is limited. Therefore, the redox properties of **poly-TThSP1** can be used to control its photochemical behavior. As expected, given the large conformational differences between spiropyrans and merocyanines, there are significant morphological changes in the polymer film, although the polymer conductivity does not appear to be dramatically affected and is similar to that of previous polythiophenes.

This unique multichromophoric and multiswitchable polymer system provides an exciting platform for the development of future materials that can exploit the other physical and chemical properties of spiropyrans and merocyanines such as variation in hydrophobicity, ion and molecular complexation, and conformational effect leading to polymer actuation. Studies to this end are underway in our laboratories.

■ ASSOCIATED CONTENT

Supporting Information. Synthesis of methyl 4,4″-didecyloxy-2,2′:5′,2″-terthiophene-3′-acetate (**TThMA**), 4,4″-didecyloxy-2,2′:5′,2″-terthiophene-3′-acetic acid (**TThAA**), and 2-(3,3″-dimethylindoline-6′-nitrobenzospiropyranyl)ethyl 4,4″-didecyloxy-2,2′:5′,2″-terthiophene-3′-acetate (**TThSP1**), electrochemical polymerization of **TThSP1** and **TThMA**, UV−vis spectroelectrochemistry, SEM and AFM imaging details and AFM images, conductivity measurements, and a movie file showing the color changes associated with the CV scan of **poly-TThSP1**. This material is available free of charge via the Internet at http://pubs.acs.org.

■ AUTHOR INFORMATION

Corresponding Author
davido@uow.edu.au

■ ACKNOWLEDGMENT

Financial support from the Australian Research Council and funding from Science Foundation Ireland under award 07/CE/I1147 "CLARITY: Centre for Sensor Web Technologies" are gratefully acknowledged.

■ REFERENCES

(1) Browne, W. R.; Feringa, B. L. *Annu. Rev. Phys. Chem.* **2009**, *60*, 407–428.
(2) Fischer, E.; Hirshberg, Y. *J. Chem. Soc.* **1952**, 4522–4524.
(3) Duerr, H., Bouas-Laurent, H., Eds. *Studies in Organic Chemistry 40: Photochromism: Molecules and Systems*; Elsevier: Amsterdam, 1990.
(4) Preigh, M. J.; Stauffer, M. T.; Lin, F.-T.; Weber, S. G. *J. Chem. Soc., Faraday Trans.* **1996**, *92*, 3991–3996.
(5) Berkovic, G.; Krongauz, V.; Weiss, V. *Chem. Rev.* **2000**, *100*, 1741–1753.
(6) Willner, I.; Willner, B. *J. Mater. Chem.* **1998**, *8*, 2543–2556.
(7) Willner, I.; Willner, B. *Bioelectrochem. Bioenerg.* **1997**, *42*, 43–57.
(8) Scarmagnani, S.; Walsh, Z.; Slater, C.; Alhashimy, N.; Paull, B.; Macka, M.; Diamond, D. *J. Mater. Chem.* **2008**, *18*, 5063–5071.
(9) Katsonis, N.; Lubomska, M.; Pollard, M. M.; Feringa, B. L.; Rudolf, P. *Prog. Surf. Sci.* **2007**, *82*, 407–434.
(10) Seki, T.; Ichimura, K. *Macromolecules* **1990**, *23*, 31–35.
(11) Byrne, R. J.; Stitzel, S. E.; Diamond, D. *J. Mater. Chem.* **2006**, *16*, 1332–1337.
(12) Lee, J.; Kwon, T.; Kim, E. *Tetrahedron Lett.* **2006**, *48*, 249–254.
(13) Wesenhagen, P.; Areephong, J.; Fernandez Landaluce, T.; Heureux, N.; Katsonis, N.; Hjelm, J.; Rudolf, P.; Browne, W. R.; Feringa, B. L. *Langmuir* **2008**, *24*, 6334–6342.
(14) Hugel, T.; Holland Nolan, B.; Cattani, A.; Moroder, L.; Seitz, M.; Gaub Hermann, E. *Science* **2002**, *296*, 1103–1106.
(15) Ustamehmetoglu, B. *Polym. Adv. Technol.* **1999**, *10*, 164–168.
(16) Roncali, J. *Chem. Rev.* **1992**, *92*, 711–38.
(17) Li, Y.; Zou, Y. *Adv. Mater.* **2008**, *20*, 2952–2958.
(18) Ahn, S.-H.; Czae, M.-z.; Kim, E.-R.; Lee, H.; Han, S.-H.; Noh, J.; Hara, M. *Macromolecules* **2001**, *34*, 2522–2527.
(19) Areephong, J.; Kudernac, T.; de Jong, J. J. D.; Carroll, G. T.; Pantorott, D.; Hjelm, J.; Browne, W. R.; Feringa, B. L. *J. Am. Chem. Soc.* **2008**, *130*, 12850–12851.
(20) Park, I. S.; Jung, Y.-S.; Lee, K.-J.; Kim, J.-M. *Chem. Commun.* **2010**, *46*, 2859–2861.
(21) Gallazzi, M. C.; Castellani, L.; Marin, R. A.; Zerbi, G. *J. Polym. Sci., Part A: Polym. Chem.* **1993**, *31*, 3339–3349.
(22) Grant, D. K.; Jolley, K. W.; Officer, D. L.; Gordon, K. C.; Clarke, T. M. *Org. Biomol. Chem.* **2005**, *3*, 2008–2015.
(23) Wagner, K.; Crowe, L. L.; Wagner, P.; Gambhir, S.; Partridge, A. C.; Earles, J. C.; Clarke, T. M.; Gordon, K. C.; Officer, D. L. *Macromolecules* **2010**, *43*, 3817–3827.
(24) Gambhir, S.; Wagner, K.; Officer, D. L. *Synth. Met.* **2005**, *154*, 117–120.
(25) McCoy, C. P.; Donnelly, L.; Jones, D. S.; Gorman, S. P. *Tetrahedron Lett.* **2007**, *48*, 657–661.
(26) Campredon, M.; Giusti, G.; Guglielmetti, R.; Samat, A.; Gronchi, G.; Alberti, A.; Benaglia, M. *J. Chem. Soc., Perkin Trans. 2* **1993**, 2089–94.
(27) Zhi, J. F.; Baba, R.; Hashimoto, K.; Fujishima, A. *J. Photochem. Photobiol., A* **1995**, *92*, 91–97.
(28) Jukes, R. T. F.; Bozic, B.; Hartl, F.; Belser, P.; De Cola, L. *Inorg. Chem.* **2006**, *45*, 8326–8341.
(29) Heiligman-Rim, R.; Hirshberg, Y.; Fischer, E. *J. Phys. Chem.* **1962**, *66*, 2465–70.
(30) Hobley, J.; Malatesta, V. *Phys. Chem. Chem. Phys.* **2000**, *2*, 57–59.
(31) Roncali, J.; Garnier, F.; Lemaire, M.; Garreau, R. *Synth. Met.* **1986**, *15*, 323–331.
(32) Brancato-Buentello, K. E.; Kang, S.-J.; Scheidt, W. R. *J. Am. Chem. Soc.* **1997**, *119*, 2839–2846.
(33) van Haare, J. A. E. H.; Groenendaal, L.; Havinga, E. E.; Meijer, E. W.; Janssen, R. A. J. *Synth. Met.* **1997**, *85*, 1091–1092.
(34) Wallace, G. G., Spinks, G. M., Kane-Maguire, L. A. P., Teasdale, P. R., Eds. *Conductive Electroactive Polymers: Intelligent Materials Systems*; CRC Press: Boca Raton, FL, 1996.
(35) Gallazzi, M. C.; Toscano, F.; Paganuzzi, D.; Bertarelli, C.; Farina, A.; Zotti, G. *Macromol. Chem. Phys.* **2001**, *202*, 2074–2085.